settings and elucidating a role between obesity and dermatologic conditions.

DATA AVAILABILITY STATEMENT

This study was performed in accordance with the Declaration of Helsinki. Deidentified data requests can be submitted for consideration to the study coordinators through the corresponding author. All requests must undergo ethics approval and require formal data sharing agreements.

KEYWORDS

3D total body photography; Body mass index; Melanoma; Obesity; Screening

ORCIDs

Sam Kahler: http://orcid.org/0000-0001-7145-4673
Brigid Betz-Stablein: http://orcid.org/0000-0003-3876-501X
Fabian Lee: http://orcid.org/0009-0001-1091-8785
Joachim Torrano: http://orcid.org/0000-0002-2043-5621
Monika Janda: http://orcid.org/0000-0002-1728-8085
Clare A. Primiero: http://orcid.org/0000-0002-2944-0013
H. Peter Soyer: http://orcid.org/0000-0002-4770-561X
Dilki Jayasinghe: http://orcid.org/0000-0003-1467-7664

CONFLICT OF INTEREST

HPS is a shareholder of MoleMap NZ and e-derm consult GmbH and undertakes regular teledermatological reporting for both companies. HPS is a medical consultant for Canfield Scientific and a medical advisor for First Derm.

ACKNOWLEDGMENTS

This study was funded through the following grants: Australian Cancer Research Foundation; NHMRC Clinical Trials and Cohort Studies Grant (2001517); NHMRC Centre of Research Excellence (2006551); NHMRC Synergy Grant (2009923). We thank our staff and participants for their integral role in the development of this work.

AUTHOR CONTRIBUTIONS

Conceptualization: HPS, JT, BB-S; Data Curation: SK, FL, JT; Formal Analysis: SK, DJ; Funding Acquisition: HPS, MJ; Investigation: SK, BB-S; Methodology: SK, BBS, DJ, JT; Project Administration: MJ, CP; Resources: HPS, MJ; Supervision: HPS, BB-S; Validation: SK, DJ; Visualization: SK; Writing - Original Draft Preparation: SK, CP, BBS; Writing - Review and Editing: SK, BB-S, FL, JT, MJ, CAP, HPS, DJ

Disclaimer

The funders had no role in the design of the study; collection, analysis, or interpretation of the data; the writing of the manuscript or decision to submit it for publication.

Sam Kahler[1], Brigid Betz-Stablein[1], Fabian Lee[1], Joachim Torrano[1], Monika Janda[2], Clare Primiero[1], H. Peter Soyer[1] and Dilki Jayasinghe[2,*]

[1]Frazer Institute, Dermatology Research Centre, The University of Queensland, Brisbane, Australia; and [2]Centre for Health Services Research, Faculty of Medicine, The University of Queensland, Brisbane, Australia
[*]Corresponding author e-mail: dilki.jayasinghe@uq.edu.au

SUPPLEMENTARY MATERIAL

Supplementary material is linked to the online version of the paper at www.jidonline.org, and at https://doi.org/10.1016/j.jid.2024.06.1294.

REFERENCES

Durnin JV, Womersley J. Body fat assessed from total body density and its estimation from skinfold thickness: measurements on 481 men and women aged from 16 to 72 years. Br J Nutr 1974;32:77–97.

Koepke N, Zwahlen M, Wells JC, Bender N, Henneberg M, Rühli FJ, et al. Comparison of 3D laser-based photonic scans and manual anthropometric measurements of body size and shape in a validation study of 123 young Swiss men. PeerJ 2017;5:e2980.

Koh U, Cust AE, Fernández-Peñas P, Mann G, Morton R, Wolfe R, et al. ACEMID cohort study: protocol of a prospective cohort study using 3D total body photography for melanoma imaging and diagnosis. BMJ Open 2023;13:e072788.

Lahmann PH, Hughes MC, Williams GM, Green AC. A prospective study of measured body size and height and risk of keratinocyte cancers and melanoma. Cancer Epidemiol 2016;40:119–25.

Lauby-Secretan B, Scoccianti C, Loomis D, Grosse Y, Bianchini F, Straif K, et al. Body fatness and cancer–viewpoint of the IARC working group. N Engl J Med 2016;375:794–8.

Pantanowitz A, Cohen E, Gradidge P, Crowther NJ, Aharonson V, Rosman B, et al. Estimation of body mass index from photographs using deep Convolutional Neural Networks. Inform Med Unlocked 2021;26:100727.

Reilly SM, Saltiel AR. Adapting to obesity with adipose tissue inflammation. Nat Rev Endocrinol 2017;13:633–43.

Stenehjem JS, Veierød MB, Nilsen LT, Ghiasvand R, Johnsen B, Grimsrud TK, et al. Anthropometric factors and Breslow thickness: prospective data on 2570 cases of cutaneous melanoma in the population-based Janus Cohort. Br J Dermatol 2018;179:632–41.

R Core Team. The R project for statistical computing. Version 4.3.2. Eye Holes, https://www.r-project.org/. (accessed October 31, 2023); 2023.

Chi3l1 Knockout Mitigates Chronic Itch and Cutaneous Inflammation in Mice

Journal of Investigative Dermatology (2025) **145,** 975–979; doi:10.1016/j.jid.2024.09.013

TO THE EDITOR

CHI3L1, also known as YKL-40, is a 40-kDa glycoprotein that is overexpressed in patients with atopic dermatitis (AD) and is induced by various proinflammatory cytokines. This protein interacts with multiple receptors (He et al, 2013; Lee et al, 2016), and its serum levels corelate with the severity of AD in humans. CHI3L1 regulates T helper type 2 cytokines and modulates IgE release (Curtiss et al, 2023; Lee et al, 2022). Antibody therapy targeting CHI3L1 has been shown to improve skin inflammation in AD in mice (Lee et al, 2022; Yu et al, 2024). CHI3L1 also activates IL-13Rα2 (Kwak et al, 2019). Although IL-13Rα2 was traditionally considered as a decoy receptor, our studies have revealed its crucial role in AD-associated itch, with increased expression observed in patients with AD (Xiao et al, 2021). Despite these findings, the role of CHI3L1 in chronic itch sensation remains largely unexplored. This study aims to elucidate the role of CHI3L1 in itch by investigating its interactions with IL-13Rα2 and IL-31 receptor, which are key itch receptors (Meng et al, 2018). In addition, our study explored the function and the effects of *CHI3L1* gene knockout (KO) on itch generation and related signaling pathways.

Abbreviations: AD, atopic dermatitis; KO, knockout; OSM, oncostatin M; WT, wild-type

Accepted manuscript published online 3 October 2024; corrected proof published online 2 November 2024

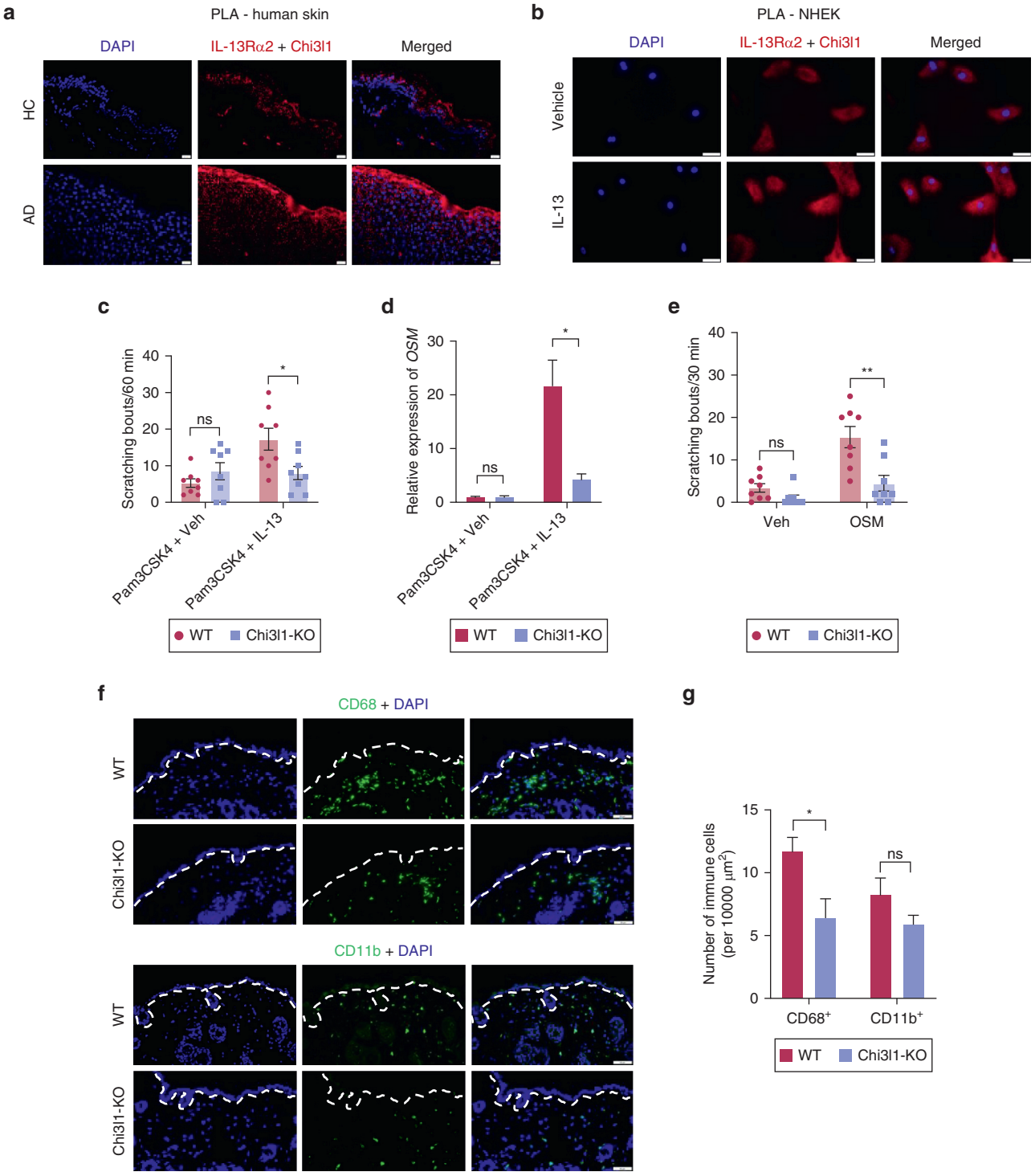

Figure 1. The CHI3L1 and IL-13Rα2 protein complexes are elevated in AD skin and NHEKs upon IL-13 stimulation. Knockout of the *Chi3l1* gene in mice results in decreased transcription of OSM and mitigates acute itch promoted by both IL-13 and OSM. **(a, b)** Representative images from PLA showing CHI3L1–IL-13Rα2 complexes in (**a**) human HC and AD skin and in (**b**) cultured NHEKs treated with or without IL-13. Nuclei are counterstained with DAPI (blue). Negative controls for PLA, in which IL-13Rα2 antibody was omitted, are shown in Supplementary Figure S1. Bar = 20 μm for **a** and 50 μm for **b**. **(c)** Comparison of itch-like behavior over a 60-min period between WT and *Chi3l1*-KO mice in response to orally administrated Pam3CSK4 followed by intradermal injection of IL-13 or vehicle. n = 8 mice per group. **(d)** RT-qPCR analysis of *OSM* mRNA in *Chi3l1*-KO mice versus WT mice in skin harvested after oral administration of Pam3CSK4 and subsequent intradermal injection of IL-13 or vehicle. n ≥ 4 mice per group. **(e)** Comparison of itch-like behavior over a 30-min period between WT and *Chi3l1*-KO mice in response to intradermal injection of OSM or vehicle. n = 8 mice per group. **(f)** Representative images and (**g**) quantification analysis of immune cell infiltration, identified by antibodies against CD68 and CD11b, in OSM-injected skin from *Chi3l1*-KO versus WT mice. n = 3 mice per group analyzed. Bar = 20 μm. Data are presented as mean ± SEM. N.S. denotes $P > .05$. *$P < .05$ and **$P < .01$, as determined by 1-way ANOVA. AD, atopic dermatitis; HC, healthy control; KO, knockout; min, minute; NHEK, normal human epidermal keratinocyte; ns, not significant; OSM, oncostatin M; PLA, proximity ligation assay; WT, wild-type.

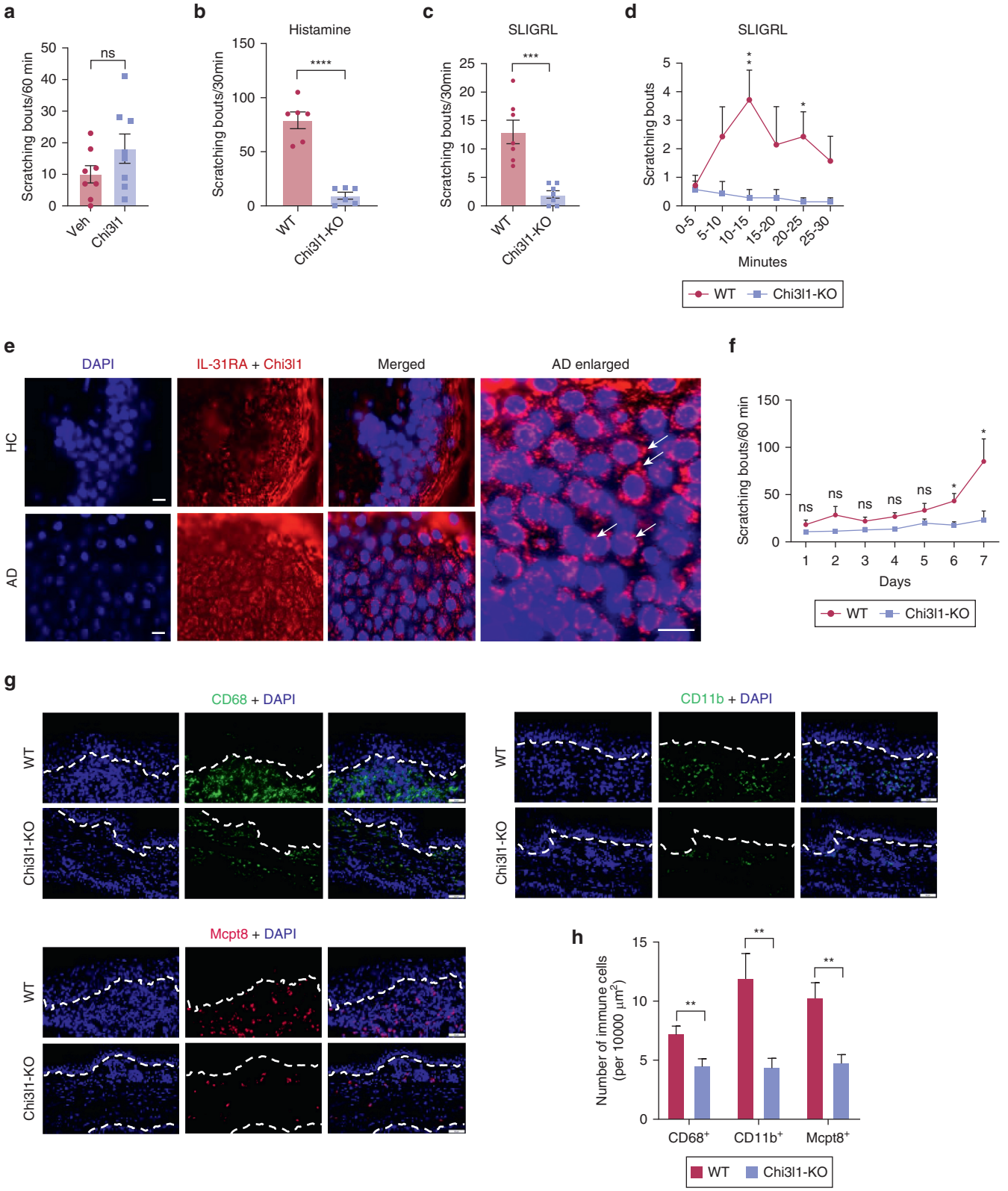

Figure 2. Intradermal injection of murine CHI3L1 protein failed to induce itch-like behavior in a mouse cheek model; scratching bouts triggered by intradermal injection of histamine and SLIGRL-NH2 are abolished in *Chi3l1*-KO mice. PLA results show that CHI3L1−IL-31RA complexes are more abundant in human lesional AD skin than in HC; *Chi3l1* knockout alleviates itch and skin inflammation in an MC903-challenged murine model of AD. **(a)** Acute itch response was not observed in WT mice after intradermal cheek injection of murine CHI3L1 compared with that in the vehicle control. n = 8 mice per group. **(b)** Comparison of histamine-induced itch-like behavior between *Chi3l1*-KO mice and WT mice. n = 6 mice per group. **(c, d)** Effect of intradermal injection of SLIGRL-NH2 on *Chi3l1*-KO mice and WT mice: (**c**) scratching bouts and (**d**) time course of itch-like response. n = 7 mice per group. **(e)** Representative PLA images showing CHI3L1−IL-31RA complexes in human lesional AD and HC. An enlarged image of AD highlights positive signals, indicated by arrows. Nuclei are counterstained with DAPI (blue). Bar = 20 μm. **(f)** Comparison of MC903-induced itch-like behavior between *Chi3l1*-KO and WT mice. n = 6 mice per

A previous study reported elevated *Chi3l1* transcription levels in the MC903-induced mouse model of AD (Walsh et al, 2019). In our current investigation, we explored the alteration of CHI3L1 and IL-13Rα2 interactions under AD conditions using proximity ligation assay, a highly sensitive method for detecting protein interactions in situ. Our results revealed that CHI3L1–IL-13Rα2 protein complexes, indicated by discrete red fluorescence spots, were increased in lesional AD skin in humans compared with that in healthy individual, predominantly in the epidermis, with fewer signals in the dermis (Figure 1a). This increase was absent in the negative controls (Supplementary Figure S1a). This alternation appeared to be associated with elevated IL-13 levels in AD skin, as demonstrated by the increased CHI3L1 and IL-13Rα2 complexes observed in cultured human primary keratinocytes upon IL-13 stimulation (Figure 1b), with no signals detected in the negative controls (Supplementary Figure S1b). These findings suggest a potential role for CHI3L1 in AD-associated skin pathology, with its interaction with IL-13Rα2 possibly being induced by the itch-promoting cytokine IL-13.

To investigate the role of CHI3L1 in IL-13–related itch, a mechanism implicated in AD, we examined *Chi3l1*-KO mice in response to IL-13–promoted itch and compared with age-matched wild-type (WT) mice. Although IL-13 alone did not significantly increase itch bouts above basal levels, it enhanced the itch response to other pruritogens (Xiao et al, 2021). Supporting this, our previous research demonstrated that oral administration of Pam3CSK4 (a toll-like receptor R2/toll-like receptor 1 agonist) before IL-13 injection into the mouse cheek significantly increased scratching bouts compared to IL-13 injection alone (Xiao et al, 2021). In this study, using the oral Pam3CSK4-enhanced IL-13–injection cheek model, we observed a significant reduction in site-directed scratching bouts, indicative of an itch-like response, in *Chi3l1*-KO compared with that in WT mice (Figure 1c). In contrast, no difference in scratching bouts was observed in the WT group (Figure 1c), suggesting a potential regulatory role of CHI3L1 in IL-13–promoted itch. In addition, RT-qPCR analysis of skin from mice treated with oral Pam3CSK4 followed by IL-13 injection revealed upregulation of the *Osm* gene in WT mice, which was attenuated in *Chi3l1*-KO mice (Figure 1d). The *Osm* gene encodes oncostatin M (OSM), an inflammatory factor known to elicit itch in mice, although with a delayed effect (Tseng and Hoon, 2021). Our findings suggest that CHI3L1 may modulate the itch signaling molecule OSM, potentially in conjunction with IL-13.

We further examined whether OSM-induced itch could be attenuated in *Chi3l1*-KO mice. Compared with vehicle injection, which resulted in minimal scratching bouts, OSM injection significantly increased scratching behavior in WT mice, with a marked reduction observed in *Chi3l1*-KO mice (Figure 1e). Immunocytochemical analysis of cheek skin 4 hours after OSM injection revealed a significant reduction in the infiltration of $CD68^+$ monocyte lineage cells and a trend toward decreased $CD11b^+$ myeloid-lineage cells in *Chi3l1*-KO compared with that in WT mice (Figure 1f and g), with no signals observed in negative control staining (Supplementary Figure S2). These findings suggest that CH3L1 plays a role in OSM-induced itch transmission and cutaneous inflammation.

To determine whether CHI3L1 can directly induce itch, we used an acute itch model involving cheek injections in mouse. Compared with the vehicle control, injection of bioactive murine CHI3L1 did not significantly increase site-directed scratching bouts, although there was a trend toward increased scratching (Figure 2a). These results suggest that CHI3CL1 may not act as a direct itch inducer on its own at the tested dose.

To further explore the role of CHI3L1 in itch, we assessed the response to histamine in the mouse cheek model. Histamine-induced scratching bouts were nearly abolished in *Chi3l1*-KO mice compared with those in WT mice (Figure 2b), confirming that CHI3L1 modulates histamine-dependent itch. We also evaluated the itch response to SLIGRL-NH2, an agonist of proteinase-activated receptor 2, a key itch receptor, in the cheek model. This revealed a significant reduction in proteinase-activated receptor 2–mediated itch in *Chi3l1*-KO mice compared with that in WT mice, as evidenced by a decrease in total scratching bouts (Figure 2c), with maximal inhibition observed between 10 and 15 minutes (Figure 2d).

To explore the involvement of CHI3L1 in AD-related itch, we examined the potential formation of CHI3L–IL-31RA complexes using proximity ligation assay. The abundance of these complexes appeared higher in AD samples than in healthy control (Figure 2e), suggesting that CHI3L1 may also signal through the IL-31 pathway, which plays a critical role in generating itch in AD.

We then established an AD-like model using topical MC903, acknowledging that this model differs from human AD in its inflammation profile. No differences were observed between *Chi3l1*-KO and WT mice during the early stages of MC903 application (days 1–5). However, by days 6–7, when the model is established, and itch intensity increases, scratching bouts were nearly abolished in *Chi3l1*-KO mice (Figure 2f).

In addition, immunohistochemical analysis revealed significantly fewer immune cell infiltrations in the MC903-treated ear of *Chi3l1*-KO than in WT mice, as indicated by staining with antibodies against CD68, CD11b, and the basophil marker Mcpt8 (Figure 2g and h), contrasting to negative controls (Supplementary Figure S2). These findings suggest that CHI3L1 contributes to both itch and cutaneous inflammation in AD.

Overall, our study unveils a previously unreported role of CHI3L1 in mediating both chronic and acute itch in mice as well as cutaneous inflammation likely through mechanisms involving IL-13Rα2, IL-31RA, and OSM. Further studies are needed to determine whether

group. **(g)** Representative images and (**h**) quantification analysis of immune cell infiltration, labeled with antibodies against CD68, CD11b, and Mcpt8 in *Chi3l1*-KO and WT mice. Bar = 20 μm. n = 3 mice per group was analyzed. Data are presented as mean ± SEM. N.S. denotes $P > .05$. *$P < .05$, **$P < .01$, ***$P < .001$, and ****$P < .0001$, as determined by Student's *t*-test. AD, atopic dermatitis; HC, healthy control; KO, knockout; ns, not significant; PLA, proximity ligation assay; WT, wild-type.

these findings extend to other models of allergic inflammation or pruritus.

ETHICS STATEMENT

The human skin tissues were purchased from Tissue Solutions (Glasgow, United Kingdom); thus, institutional approval and patient consent were not necessary. All animal procedures were performed in accordance with the Guidelines for Care and Use of Laboratory Animals of Henan University and approved by the Animal Ethics Committee of Henan University (Henan, China).

DATA AVAILABILITY STATEMENT

All data generated or analyzed during this study are included in the manuscript.

KEYWORDS

Atopic dermatitis; IL-13; IL-31; PAR2; TLR2

ORCIDs

Xingyun Zhu: http://orcid.org/0009-0004-3368-6755
Xiaolong Dai: http://orcid.org/0000-0002-6478-5252
Weiwei Chen: http://orcid.org/0000-0002-1965-7606
Yanqing Li: http://orcid.org/0000-0002-4406-7878
Yang Liu: http://orcid.org/0000-0002-1335-0531
Chunxu Shan: http://orcid.org/0000-0001-8670-0208
Jiafu Wang: http://orcid.org/0000-0002-3654-4400
Jianghui Meng: http://orcid.org/0000-0002-3107-4200

CONFLICT OF INTEREST

The authors state no conflict of interest.

ACKNOWLEDGMENTS

This work is supported by funding from Science Foundation Ireland (23/FFP-A/11956), the Natural Science Foundation of Henan (242300421517), and the LEO Foundation.

AUTHOR CONTRIBUTIONS

Conceptualization: JM, JW; Data Curation: XZ, XD, WC, YLi, YLiu, CS, JW, JM; Funding Acquisition: JM, JW, WC; Supervision: JM, JW; Writing - Original Draft Preparation: XZ, XD, WC, YLi, YLiu, CS, JW, JM; Writing - Review and Editing: XZ, XD, WC, YLi, YLiu, CS, JW, JM

***Xingyun Zhu*[1,3], *Xiaolong Dai*[1,3], *Weiwei Chen*[1], *Yanqing Li*[1], *Yang Liu*[1], *Chunxu Shan*[2], *Jiafu Wang*[2,4] and *Jianghui Meng*[2,4,*]**

[1]*School of Life Sciences, Henan University, Henan, China; and* [2]*School of Biotechnology, Faculty of Science and Health, Dublin City University, Dublin, Ireland*

[3]*These authors contributed equally to this study.*
[4]*These authors contributed equally as senior authors.*

[*]*Corresponding author e-mail: Jianghui.meng@dcu.ie*

SUPPLEMENTARY MATERIAL

Supplementary material is linked to the online version of the paper at www.jidonline.org, and at https://doi.org/10.1016/j.jid.2024.09.013.

REFERENCES

Curtiss ML, Rosenberg AF, Scharer CD, Mousseau B, Benavides NAB, Bradley JE, et al. Chitinase-3-like 1 regulates T_H2 cells, T_{FH} cells and IgE responses to helminth infection. Front Immunol 2023;14:1158493.

He CH, Lee CG, Dela Cruz CS, Lee CM, Zhou Y, Ahangari F, et al. Chitinase 3-like 1 regulates cellular and tissue responses via IL-13 receptor alpha2. Cell Rep 2013;4:830–41.

Kwak EJ, Hong JY, Kim MN, Kim SY, Kim SH, Park CO, et al. Chitinase 3-like 1 drives allergic skin inflammation via Th2 immunity and M2 macrophage activation. Clin Exp Allergy 2019;49:1464–74.

Lee CM, He CH, Nour AM, Zhou Y, Ma B, Park JW, et al. IL-13Ralpha2 uses TMEM219 in chitinase 3-like-1-induced signalling and effector responses. Nat Commun 2016;7:12752.

Lee YS, Yu JE, Kim MJ, Ham HJ, Jeon SH, Yun J, et al. New therapeutic strategy for atopic dermatitis by targeting CHI3L1/ITGA5 axis. Clin Transl Med 2022;12:e739.

Meng J, Moriyama M, Feld M, Buddenkotte J, Buhl T, Szöllösi A, et al. New mechanism underlying IL-31-induced atopic dermatitis. J Allergy Clin Immunol 2018;141:1677–1689.e8.

Tseng PY, Hoon MA. Oncostatin M can sensitize sensory neurons in inflammatory pruritus. Sci Transl Med 2021;13:eabe3037.

Walsh CM, Hill RZ, Schwendinger-Schreck J, Deguine J, Brock EC, Kucirek N, et al. Neutrophils promote CXCR3-dependent itch in the development of atopic dermatitis. Elife 2019;8:e48448.

Xiao S, Lu Z, Steinhoff M, Li Y, Buhl T, Fischer M, et al. Innate immune regulates cutaneous sensory IL-13 receptor alpha 2 to promote atopic dermatitis. Brain Behav Immun 2021;98:28–39.

Yu JE, Jeon SH, Kim MJ, Kim DH, Koo JK, Kim TH, et al. Anti-chitinase-3-like 1 antibody attenuated atopic dermatitis-like skin inflammation through inhibition of STAT3-dependent CXCL8 expression. Br J Pharmacol 2024;181:3232–45.

Combined Inhibition of MNK Signaling and BET Proteins Reveals TGM2 as a Novel Vulnerability in Melanoma

Journal of Investigative Dermatology (2025) **145,** 979–984; doi:10.1016/j.jid.2024.07.037

TO THE EDITOR

The successes of targeted therapies against *BRAF*-mutated melanoma and immune checkpoint inhibitors are limited by resistance mechanisms, highlighting the need to develop new treatment strategies. MNK1/2 inhibitors target a nexus point of the MAPK signaling cascades and have shown efficient antitumor effects in melanoma when combined with standard-of-care therapeutics, representing a promising treatment option (Huang et al, 2021; Prabhu et al, 2023). Bromo- and extra-terminal domain (BET) proteins are transcriptional coactivators that enhance the transcriptional elongation of many oncogenes in numerous cancers (Shorstova et al, 2021). In melanoma, BET family members BRD2 and BRD4 are overexpressed compared with those in benign nevi (Segura et al, 2013), suggesting a link with melanoma growth and progression. Consistent with this,

Abbreviations: A375-VR, vemurafenib-resistant A375; BET, bromo- and extra-terminal domain; BETi, bromo- and extra-terminal domain inhibitor; ECM, extracellular matrix; FAK, focal adhesion kinase; MAPKi, MAPK inhibitor

Accepted manuscript published online 1 October 2024; corrected proof published online 28 October 2024

SUPPLEMENTARY METHOD AND MATERIALS

Animals

All C57BL/6 mice were obtained from SPF Biotechnology, and *Chi3l1*-knockout mice were purchased by Cyagen Biosciences. These mice were bred in house. All experiments were conducted using female mice aged 6−8 weeks. Animal procedures adhered to the Guidelines for the Care and Use of Laboratory Animals of Henan University and were approved by the Animal Ethics Committee of Henan University.

Human samples

Human skin biopsies for immunohistochemistry were commercially purchased from Tissue Solutions. These paraffin-embedded samples were donated by either patients or healthy individuals. No ethical approval was requested for the use of these samples.

Culture and stimulation of primary human keratinocytes

Primary human keratinocytes were seeded into IBIDI chambers and cultured in KBM-Gold medium supplemented with KBM Gold SingleQuot KC supplement (Lonza). Cells were incubated in the medium for 3 days before performing proximity ligation assay experiments.

Prior to proximity ligation assays, primary human keratinocytes were maintained in hydrocortisone-free medium for ≥24 hours and stimulated with hydrocortisone-free media ± IL-13 (100 ng/ml, 24 hours, AB270080, Abcam).

Immunofluorescence staining

Paraffin sections of mouse skin were deparaffinized and rehydrated, followed by antigen retrieval and permeabilization (Triton X-100 [0.2%], PBS). Sections were then incubated in a blocking solution (normal goat serum [5%], PBS) for 1 hour. Subsequently, specimens were incubated (4 °C, overnight) with primary antibodies in blocking solution: CD68 (AB283654, Abcam, 1:100), CD11b (AB133357, Abcam, 1:500), and Mcpt8 (647401, BioLegend, 1:500). Next, specimens were washed (PBS) and incubated with anti-rabbit (Alexa 488, goat) and/or anti-rat (Alexa 594, goat). After washing (PBS), the specimens were mounted using ProLong anti-fade reagent containing DAPI (Thermo Fisher Scientific). Images were captured by an IX73 Olympus inverted microscope with CellSens Dimension Imaging software.

Proximity ligation assay

Paraffin sections of human skin were deparaffinized, rehydrated, subjected to antigen retrieval, and permeabilized (Triton X-100 [0.2%], PBS). Cultured primary human keratinocytes treated with or without IL-13 (ab270080, Abcam, 100 ng/ml) were fixed and permeabilized (Triton X-100 [0.1%], PBS). The interaction between IL-13Rα2 and CHI3L1 was visualized as red fluorescent dots using the Duolink proximity ligation assay kit (DUO92002, DUO92004, DUO92008, DUO82049, Sigma-Aldrich), following the manufacturer's instructions and our previous established procedure (Meng et al, 2016). The following pairs of primary antibodies were used: rabbit anti−IL-13Rα2 (PA5-96045, Thermo Fisher Scientific, 1:200) paired with mouse anti-CHI3L1 (MA5-36122, Thermo Fisher Scientific, 1:100) or rabbit anti−IL-31RA (PA5121824, Thermo Fisher Scientific, 1:100) paired with mouse anti-CHI3L1 (MA5-36122, Thermo Fisher Scientific, 1:100). After the incubation with proximity ligation assay probes, the ligation, and amplification steps, the specimens were mounted with Fluoroshield containing DAPI (F6057, Sigma-Aldrich) to stain cell nuclei. Negative controls were performed by omitting either the IL-13Rα2 or IL-31RA antibody.

Intradermal cheek injection model

Chi3l1-knockout and wild-type C57BL/6 mice were preadministered with Pam3CSK4 (20 μg/100 μl in sterilized water) by gavage every 3 days for a total of 3 times. After this, the mice received intradermal injections of IL-13 (1 μg/10 μl) or vehicle (10 μl, sterilized water) into the right cheek (Xiao et al, 2021). All mice were video recorded for 60 minutes to analyze scratching bouts, with bouts of hind limb scratches directed at the injection site being considered indicative of pruritus (Kido-Nakahara et al, 2014; LaMotte et al, 2011).

In another experiment, *Chi3l1*-knockout and wild-type C57BL/6 mice (aged 6−8 weeks) received intradermal injections of oncostatin M (495-MO-025/CF, R&D Systema, 100 ng, 5 μl) or vehicle (PBS, 5 μl) into the right cheek (Chen et al, 2022). The resulting behavioral responses were recorded for 30 minutes.

In a separate set of experiment, wild-type C57BL/6 mice (aged 6−8 weeks) received intradermal injections of CHI3L1 (HY-P76702, MedChemExpress, 500 ng, 10 μl) or vehicle (sterilized water, 10 μl) into the right cheek. Behavioral responses were recorded for 60 minutes.

To evaluate the effect of histamine- or SLIGRL-NH2−induced itch-like response, histamine (50 μg/10 μl) dissolved in sterile saline containing 7% Tween 80 or SLIGRL-NH2 (50 μg/10 μl, Sigma-Aldrich) dissolved in Tyrode's solution (137 mM sodium chloride, 2.7 mM potassium chloride, 1.0 mM magnesium chloride, 1.8 mM calcium chloride, 20 mM 4-[2-hydroxyethyl]-1-piperazineethanesulfonic acid, 5.6 mM glucose, pH 7.4) was injected into the right cheek, and all the mice were video recorded for 30 minutes to analyze scratching bouts. Results were compared with those of their vehicle-injected mice.

In some cases, cheek skin samples from the injected mice were harvested 4 hours after injection for further analysis. These samples were either processed for immunohistochemical staining after paraffin embedding and sectioning or used for RT-qPCR analysis. For the latter, high-quality RNA was extracted using TRIzol reagent (15596026, Invitrogen) after homogenization by grinding on liquid nitrogen.

MC903-treated atopic dermatitis−like mouse model

Chi3l1-knockout and wild-type C57BL/6 mice (aged 6−8 weeks) were treated daily with a topical application of MC903 (2 nmol, 20 μl in ethanol, Sigma-Aldrich) on one ear, whereas the vehicle (ethanol, 20 μl) was applied to the opposite ear, respectively (Larkin et al, 2021). Mice were continually video recorded for 60 minutes to analyze scratching bouts. On day 7, the mice were killed, and the ear skin was photographed, collected, processed, and embedded in paraffin for subsequent immunohistochemical analysis.

RNA isolation and RT-qPCR

Total RNA was isolated from murine skin using the Nucleospin RNA Midi kit (74104, Qiagen), following the manufacturer's instructions. RNA concentration was determined using a Nanodrop 2000 spectrophotometer (Thermo Fisher Scientific). cDNA was synthesized from mRNA transcripts using a high-capacity cDNA reverse transcription kit (4368814, Thermo Fisher Scientific), with 1 μg of total RNA reverse transcribed into cDNA. RT-qPCR was performed by incubating the cDNAs with SYBR Green PCR Master mix (4309155, Thermo Fisher Scientific) and specific primers, with GAPDH used for normalizatioen. The primers for murine oncostatin M were CAATCGTGGCTGCTCCAACTCT (forward) and GGTGTGTTCAGGTTTTG GAGGC (reverse).

Data analysis

Data are presented as mean ± SEM and analyzed using Prism (GraphPad Software). Comparisons between 2 groups were made using a 2-tailed Student's *t*-test followed by Welch's correction, and *P*-values <.05 are considered statistically significant. Itch-like behavior data were presented as means ± SEMs (n ≥6 mice per group). Statistical significance was indicated by $*P < .05$, $**P < .01$, and $***P < .001$, in Student's *t*-test or 1-way ANOVA.

SUPPLEMENTARY REFERENCES

Chen W, Li Y, Steinhoff M, Zhang W, Buddenkotte J, Buhl T, et al. The PLAUR signaling promotes chronic pruritus. FASEB J 2022;36:e22368.

Kido-Nakahara M, Buddenkotte J, Kempkes C, Ikoma A, Cevikbas F, Akiyama T, et al. Neural peptidase endothelin-converting enzyme 1 regulates endothelin 1-induced pruritus. J Clin Invest 2014;124:2683–95.

LaMotte RH, Shimada SG, Sikand P. Mouse models of acute, chemical itch and pain in humans. Exp Dermatol 2011;20:778–82.

Larkin C, Chen W, Szabó IL, Shan C, Dajnoki Z, Szegedi A, et al. Novel insights into the TRPV3-mediated itch in atopic dermatitis. J Allergy Clin Immunol 2021;147:1110–1114.e5.

Meng J, Wang J, Steinhoff M, Dolly JO. TNFalpha induces co-trafficking of TRPV1/TRPA1 in VAMP1-containing vesicles to the plasmalemma via Munc18-1/syntaxin1/SNAP-25 mediated fusion. Sci Rep 2016;6:21226.

Xiao S, Lu Z, Steinhoff M, Li Y, Buhl T, Fischer M, et al. Innate immune regulates cutaneous sensory IL-13 receptor alpha 2 to promote atopic dermatitis. Brain Behav Immun 2021;98:28–39.

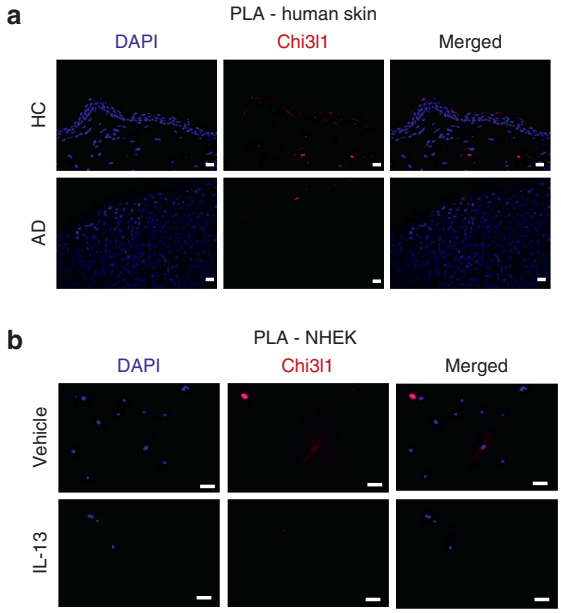

Supplementary Figure S1. Representative images of negative control staining where the IL-13Rα2 antibody was omitted from the PLA corresponding to Figure 1. Figure shows no CHI3L1—IL-13Rα2 complexes in (**a**) human HC and AD skin and in (**b**) cultured phKCs treated with or without IL-13. Nuclei are counterstained with DAPI (blue). Bars = 20 μm for a and 50 μm for b. AD, atopic dermatitis; HC, healthy control; NHEK, normal human epidermal keratinocyte; phKC, primary human keratinocyte; PLA, proximity ligation assay.

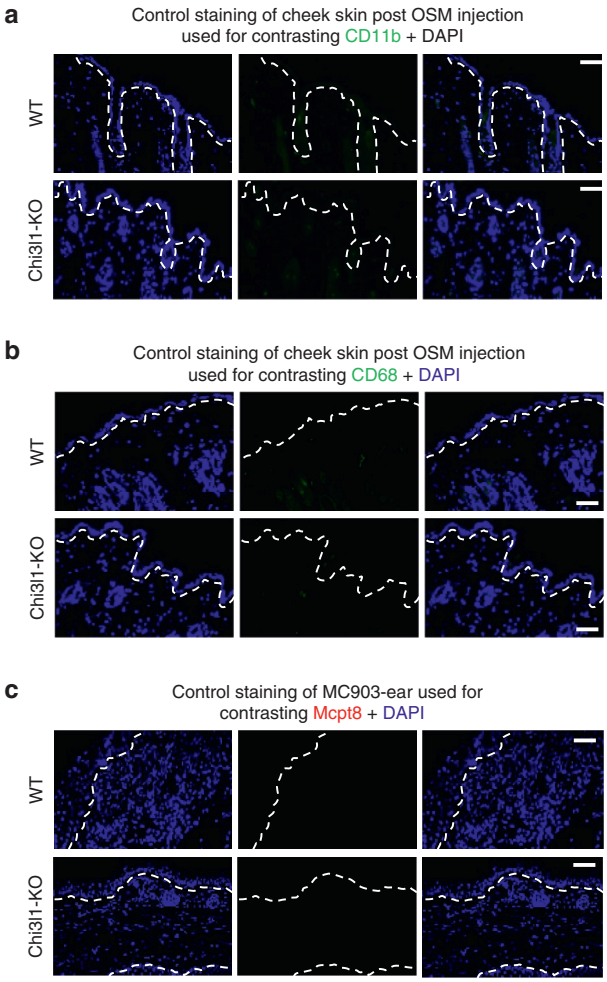

Supplementary Figure S2. Representative images of isotype control staining. **(a, b)** Isotype staining of OSM-injected skin in *Chi3l1*-KO mice and WT mice, used for contrasting (**a**) anti-CD11b and (**b**) anti-CD68 staining. **(c)** MC903-treated ear stained by isotype IgG, used for contrasting anti-Mcpt8 staining. Bar = 20 μm. KO, knockout; OSM, oncostatin M; WT, wild-type.